SISSA

Long-term performance and longevity studies of the CMS Resistive Plate Chambers

To cite this article: R.I. Rabadan-Trejo *et al* 2018 *JINST* **13** P08024

View the article online for updates and enhancements.

Long-term performance and longevity studies of the CMS Resistive Plate Chambers

R.I. Rabadan-Trejo,[w,1] **A. Fagot,**[a] **M. Gul,**[a] **C. Roskas,**[a] **M. Tytgat,**[a] **N. Zaganidis,**[a]

S. Fonseca De Souza,[b] **A. Santoro,**[b] **F. Torres Da Silva De Araujo,**[b] **A. Aleksandrov,**[c]

R. Hadjiiska,[c] **P. Iaydjiev,**[c] **M. Rodozov,**[c] **M. Shopova,**[c] **G. Sultanov,**[c] **A. Dimitrov,**[d] **L. Litov,**[d]

B. Pavlov,[d] **P. Petkov,**[d] **A. Petrov,**[d] **S.J. Qian,**[e] **D. Han,**[f] **W. Yi,**[f] **C. Avila,**[g] **A. Cabrera,**[g]

C. Carrillo,[g] **M. Segura,**[g] **S. Aly,**[h] **Y. Assran,**[h] **A. Mahrous,**[h] **A. Mohamed,**[h] **C. Combaret,**[i]

M. Gouzevitch,[i] **G. Grenier,**[i] **F. Lagarde,**[i] **I.B. Laktineh,**[i] **H. Mathez,**[i] **L. Mirabito,**[i]

K. Shchablo,[i] **I. Bagaturia,**[j] **D. Lomidze,**[j] **I. Lomidze,**[j] **L.M. Pant,**[k] **V. Bhatnagar,**[l] **R. Gupta,**[l]

R. Kumari,[l] **M. Lohan,**[l] **J.B. Singh,**[l] **V. Amoozegar,**[m] **B. Boghrati,**[m,n] **H. Ghasemy,**[m]

S. Malmir,[m] **M. Mohammadi Najafabadi,**[m] **M. Abbrescia,**[o] **A. Gelmi,**[o] **G. Iaselli,**[o] **S. Lezki,**[o]

G. Pugliese,[o] **L. Benussi,**[p] **S. Bianco,**[p] **D. Piccolo,**[p] **F. Primavera,**[p] **S. Buontempo,**[q]

A. Crescenzo,[q] **G. Galati,**[q] **F. Fienga,**[q] **I. Orso,**[q] **L. Lista,**[q] **S. Meola,**[q] **P. Paolucci,**[q]

E. Voevodina,[q] **A. Braghieri,**[r] **P. Montagna,**[r] **M. Ressegotti,**[r] **C. Riccardi,**[r] **P. Salvini,**[r]

P. Vitulo,[r] **S. W. Cho,**[s] **S. Y. Choi,**[s] **B. Hong,**[s] **K. S. Lee,**[s] **J. H. Lim,**[s] **S. K. Park,**[s] **J. Goh,**[t,aa]

T. J. Kim,[t] **S. Carrillo Moreno,**[u] **O. Miguel Colin,**[u] **F. Vazquez Valencia,**[u]

S. Carpinteyro Bernardino,[v] **J. Eysermans,**[v] **I. Pedraza,**[v] **C. Uribe Estrada,**[v]

R. Reyes-Almanza,[w] **M.C. Duran-Osuna,**[w] **M. Ramirez-Garcia,**[w] **G. Ramirez-Sanchez,**[w]

A. Sanchez-Hernandez,[w] **H. Castilla-Valdez,**[w] **A. Radi,**[x] **H. Hoorani,**[y] **S. Muhammad,**[y]

M.A. Shah[y] **and I. Crotty**[z] **on behalf of the CMS collaboration**

[a]*Ghent University, Department of Physics and Astronomy, Proeftuinstraat 86, B-9000 Ghent, Belgium*

[b]*Departamento de Fisica Nuclear e Altas Energias, Instituto de Fisica,*
Universidade do Estado do Rio de Janeiro,
Rua Sao Francisco Xavier, 524, BR - Rio de Janeiro 20559-900, RJ, Brazil

[c]*Bulgarian Academy of Sciences, Institute for Nuclear Research and Nuclear Energy,*
Tzarigradsko shaussee Boulevard 72, BG-1784 Sofia, Bulgaria

[d]*Faculty of Physics, University of Sofia, 5 James Bourchier Boulevard, BG-1164 Sofia, Bulgaria*

[e]*School of Physics, Peking University, Beijing 100871, China*

[f]*Tsinghua University, Shuangqing Rd, Haidian Qu, Beijing, China*

[g]*Universidad de Los Andes, Apartado Aereo 4976, Carrera 1E, no. 18A 10, CO-Bogota, Colombia*

[h]*Egyptian Network for High Energy Physics, Academy of Scientific Research and Technology,*
101 Kasr El-Einy St. Cairo Egypt

---

[1]Corresponding author.

^{i}*Universite de Lyon, Universite Claude Bernard Lyon 1, CNRS-IN2P3,*
Institut de Physique Nucleaire de Lyon,
Villeurbanne, France

^{j}*Georgian Technical University, 77 Kostava Str., Tbilisi 0175, Georgia*

^{k}*Nuclear Physics Division Bhabha Atomic Research Centre, Mumbai 400 085, India*

^{l}*Department of Physics, Panjab University, Chandigarh Mandir 160 014, India*

^{m}*School of Particles and Accelerators, Institute for Research in Fundamental Sciences (IPM), Tehran, Iran*

^{n}*School of Engineering, Damghan University, Damghan, Iran*

^{o}*INFN, Sezione di Bari, Via Orabona 4, IT-70126 Bari, Italy*

^{p}*INFN, Laboratori Nazionali di Frascati (LNF), Via Enrico Fermi 40, IT-00044 Frascati, Italy*

^{q}*INFN, Sezione di Napoli, Complesso Universitario Monte S. Angelo, Via Cintia, IT-80126 Napoli, Italy*

^{r}*INFN, Sezione di Pavia, Via Bassi 6, IT-Pavia, Italy*

^{s}*Korea University, Department of Physics, 145 Anam-ro, Seongbuk-gu, Seoul 02841, Republic of Korea*

^{t}*Hanyang University, 222 Wangsimni-ro, Sageun-dong, Seongdong-gu, Seoul, Republic of Korea*

^{u}*Universidad Iberoamericana, Mexico City, Mexico*

^{v}*Benemerita Universidad Autonoma de Puebla, Puebla, Mexico*

^{w}*Cinvestav, Av. Instituto Politécnico Nacional No. 2508,*
Colonia San Pedro Zacatenco, CP 07360, Ciudad de Mexico D.F., Mexico

^{x}*Sultan Qaboos University, Al Khoudh, Muscat 123, Oman*

^{y}*National Centre for Physics, Quaid-i-Azam University, Islamabad, Pakistan*

^{z}*Department of Physics, Wisconsin University, Madison, WI 53706, United States*

^{aa}*Kyunghee University, 26 Kyungheedae-ro, Hoegi-dong, Dongdaemun-gu, Seoul, Republic of Korea*

E-mail: raul.iraq.rabadan.trejo@cern.ch

ABSTRACT: Four double-gap CMS resistive plate chambers are being tested at the CERN Gamma Irradiation Facility to determine the performance and aging effects at the expected conditions of the High Luminosity-Large Hadron Collider. Results up to an integrated charge of 290 millicoulomb/cm^2 are reported.

Contents

1   Introduction

The resistive plate chambers (RPC) system, which is one of the subdetectors of the CMS muon system [1, 2] at the CERN LHC [3], provides muon triggering due to its fast response time and contributes to the muon reconstruction. RPCs will play an essential role for muon triggering at CMS during the operation of the High Luminosity Large Hadron Collider (HL-LHC) [4, 5]; therefore good performance at high luminosity is necessary for the efficient operation of CMS. The existing RPC system has operated since 2009 and will now be expected to operate throughout the data-taking period of the HL-LHC, in which it is intended to collect about $3000\,\mathrm{fb}^{-1}$ of pp collisions over 10 years of operation. However, these RPCs were originally built and validated for only ten years of LHC operation totaling $500\,\mathrm{fb}^{-1}$. During the early years of LHC operation the RPC group performed a variety of measurements, which are reported in [6, 7], to estimate the aging effects during the LHC luminosity of $500\,\mathrm{fb}^{-1}$.

Now that the expected luminosity and lifetime have increased it is essential to validate these RPC chambers for the new environment at the HL-LHC. Aging effects are complex, but typically the performance of the chambers is expected to deteriorate with the increase of the integrated charge deposited in the chambers, which is measured in millicoulomb/cm^2 (mC·cm^{-2}). The severity of aging increases with the radiation exposure and is correlated to many factors, such as the electrode materials, operational gas gain, gas mixture, impurities in the gas itself, gas floaw rate, etc. Signatures of possible aging effects include a rise in spurious signal rates, increase in leakage currents, and a reduction in chamber efficiency. Because of the more difficult conditions at the HL-LHC it is important to experimentally verify the performance of the RPCs in those conditions, and to estimate the performance of the RPC system during the period of HL-LHC operations.

For these reasons the RPC group has begun a series of dedicated tests at the Gamma Irradiation Facility (GIF++) [8] at CERN using 4 existing RPC chambers; two of them will be irradiated with the goal of reaching the maximum amount of integrated charge expected during HL-LHC running (about

840 mC·cm^{-2}), whereas the remaining two will be used as a reference and will not be irradiated. During this accelerated aging tests the efficiency and cluster sizes of the chambers will be measured as a function of the background irradiation rate and the integrated charge. Furthermore, hit rates, operating high voltage, and current are measured at different integrated charges and compared to the reference values from the nonirradiated chambers. Although the role that the gas system and the gas mixture play is important in aging studies, this issue is not addressed in this paper. We understand that studies in relation to the gas system and mixture are important concerns which are being studied by the RPC community. This paper presents the expected rate performance of the chambers and an early estimate of the longevity.

2 The present RPC system

The CMS Resistive Plate Chamber system [2] is a double-gap chamber with readout strips placed in the middle between the two gas gaps. Each RPC consists of two 2 mm thick resistive high pressure laminate (HPL) plates, commonly known as Bakelite; these plates are separated by a 2 mm gas gap. The RPCs chambers are operated in avalanche mode using a gas mixture of 95.2% freon (C$_2$H$_2$F$_4$), 4.5% isobutane (i-C$_4$H$_{10}$), and 0.3% sulfur hexafluoride (SF$_6$). The readout plane is located between both gaps and consist of copper strips with a pitch between 2.28 and 4.10 cm in the barrel and between 1.74 and 3.63 cm in the endcaps. The strip signals are asynchronously sent to the Front End Boards (FEBs) which shapes the signal before being sent to the RPC linkboard system and the CMS data acquisition system (DAQ).

The present RPC system consists of 480 chambers in the barrel and 576 chambers in the endcap. The RPC system is organized in four stations, RB1 to RB4 in the barrel region, and RE1 to RE4 in the endcap region. The innermost barrel stations RB1 and RB2 are instrumented with two layers of RPCs, all other RPC stations in the barrel and endcaps have one RPC chamber per station. A quadrant view of the CMS experiment is shown in figure 1.
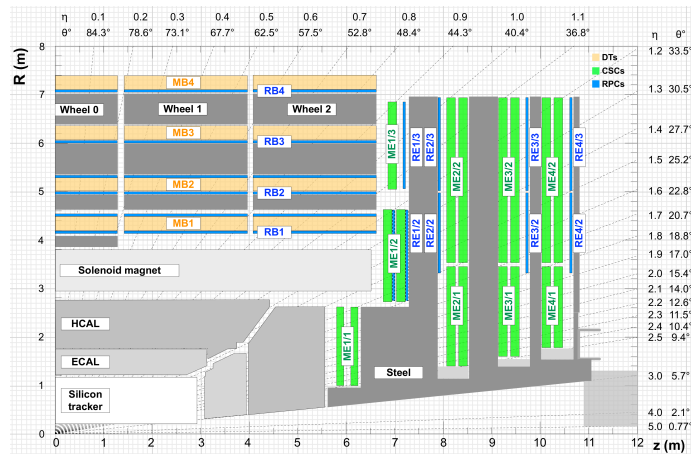

Figure 1. A quadrant of the CMS experiment. RPC stations are labeled as RB for the barrel region and RE for the endcap region.

3 Background in the muon system

Background radiation in the CMS muon system is an important factor in the performance and longevity of the detectors. A clear understanding of the background plays a crucial role not only on the performance of the existing muon system [9], but also in the design and preparation for the upgraded detector for the HL-LHC [10].

We use the raw RPC hit rate per strip to measure existing background rates during pp collisions at 7, 8 and 13 TeV [11, 12]. A linear dependence of the RPC hit rate on the LHC instantaneous luminosity is observed up to luminosities of 1.2×10^{34} cm^{-2}·s^{-1}. This linear behavior is true, not only at chamber level, but also for larger parts of the system, such as barrel wheels and endcap disks, as shown in figure 2.
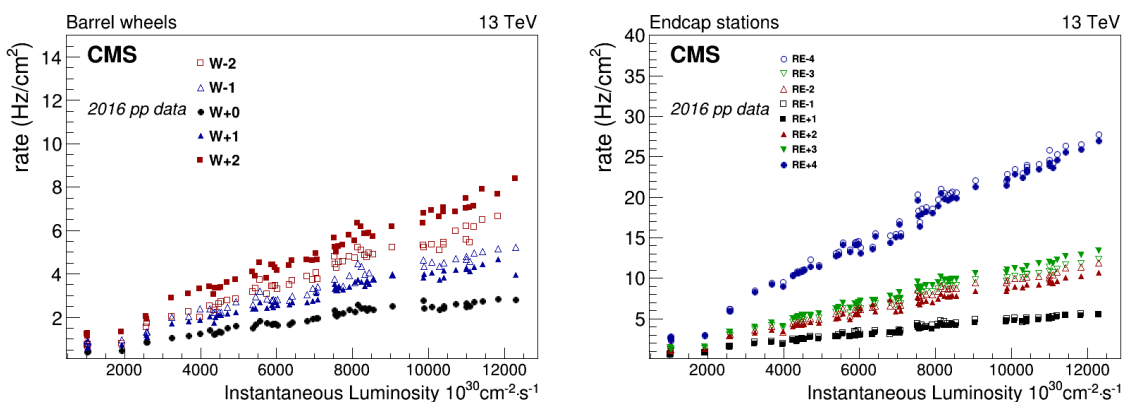

Figure 2. RPC wheels hit rate vs instantaneous luminosity (left). RPC disks hit rate vs instantaneous luminosity (right).

Based on the linear relations between rates and instantaneous luminosity, the RPC hit rates can be extrapolated to an instantaneous luminosity of 5×10^{34} cm^{-2}·s^{-1} to estimate the expected rate at the HL-LHC and also the maximum expected integrated charge on the RPC chambers by the end of the HL-LHC.

Assuming the same linear relationship holds at a luminosity of about one order of magnitude higher, the expected rates at HL-LHC conditions are shown in figure 3 for all barrel and endcap chambers. A maximum rate about 200 Hz·cm^{-2} is expected. If we apply a safety factor of three, the performance of the detector must be acceptable at a rate of 600 Hz·cm^{-2}.

The maximum expected integrated charge on the RPC chambers can be evaluated on the basis of the expected integrated luminosity at the HL-LHC, which sets an upper limit for the validation of the RPC performance. The maximum integrated charge that any chamber has received in pp collisions by the end of 2016 is about 4.2 mC·cm^{-2}, which corresponds to a luminosity of 45 fb^{-1}. By extrapolating to the expected 3000 fb^{-1} the total integrated charge by the end of the HL-LHC will be 280 mC·cm^{-2} as shown in figure 4. Including a safety factor of three, the RPCs need to be certified at GIF++ up to 840 mC·cm^{-2}.
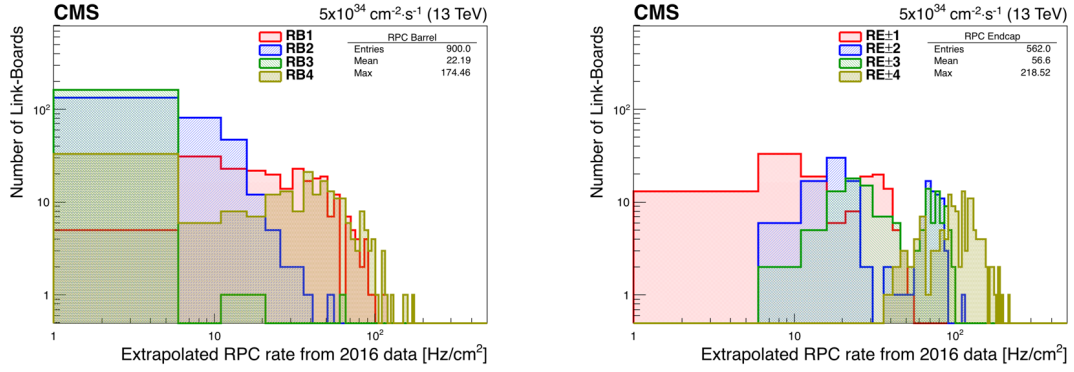
Figure 3. Expected rate extrapolated from 2016 data of single hit rate per unit area to HL-LHC conditions, in the barrel (left) and endcap (right) regions, for the present RPC system.
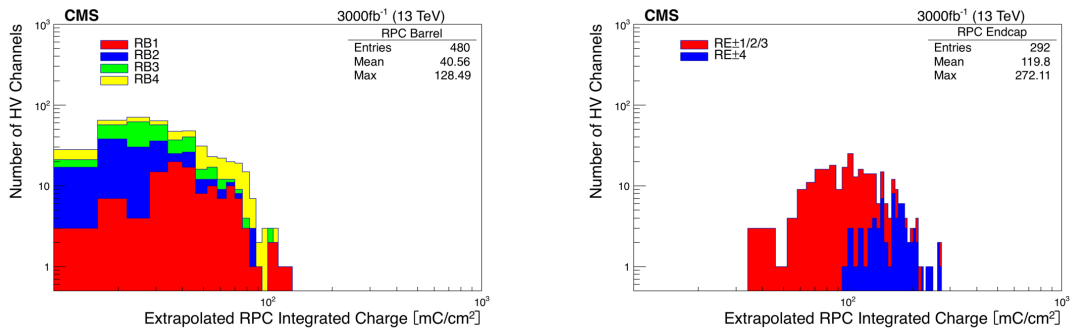

Figure 4. Expected integrated charge during the HL-LHC running ($3000\,\text{fb}^{-1}$) in the barrel (left) and endcap (right) regions, for the present RPC system.

4 GIF++ radiation facility

In order to study the longevity of RPCs in the context of the expected HL-LHC radiation doses, the GIF++ (Gamma Irradiation Facility) [8] test zone started its operation at CERN in 2015. GIF++ features an intense ^{137}Cs source of 662 KeV photons with a set of filters of various attenuation factors. As of March 2016, the intensity of the Cesium source was about 13.5 TBq. The GIF++ photons have an energy fairly representative of the energy of the LHC/HL-LHC photons seen by the muon detectors, between 0.1 MeV and 10 MeV. The source provides continuous irradiation over large areas and has sufficient room for testing several full-size muon detectors at the same time, which makes it an excellent facility for accelerated aging tests of large-size detectors.

5 Description of the GIF++ tests

Tests have been performed, or are in progress, in order to certify the present RPC system up to the expected HL-LHC conditions: integrated charge of $\sim 840\,\text{mC}\cdot\text{cm}^{-2}$ and background hit rates of $600\,\text{Hz}\cdot\text{cm}^{-2}$.

The maximum background rate is expected in the endcap regions, so in July 2016 an irradiation test was started at GIF++ using four spare endcap chambers: two RE2/2 detectors and two RE4/2

chambers. Two different types of chambers have been used for this tests because the endcap RPC production was performed in two periods: in 2005 for all RPCs in the RE1, RE2 and RE3 disks and in 2013 for the RE4/2 and RE4/3 chambers, which were installed during 2015.

To estimate the longevity of the RPCs, one RE2/2 chamber and one RE4/2 chamber are continuously operated under gamma irradiation, while the other two remaining chambers are operated only sporadically and are used as reference. The main detector parameters such as current and counting rates in several background conditions are always monitored and periodically compared with those of the reference chambers. Furthermore, when the muon beam at GIF++ is available, the detector performance, in terms of efficiency and cluster size, is measured with and without background. All measurements are performed under controlled environmental and gas conditions. The detectors are operating with the standard gas mixture (95.2% freon, 4.5% isobutane, and 0.3% SF_6), with two fresh gas volume changes per hour for the irradiated chambers and one for the reference chambers. The relative gas humidity is 40%.

A plot of the integrated charge versus time is shown in figure 5 for the RE2/2 and RE4/2 chambers. By the end of 2017, about 290 mC·cm^{-2} and 110 mC·cm^{-2} have been integrated in the RE2/2 and RE4/2 detectors, respectively. The charge integrated so far on RE2/2 is about one-third of the total integrated charge target.
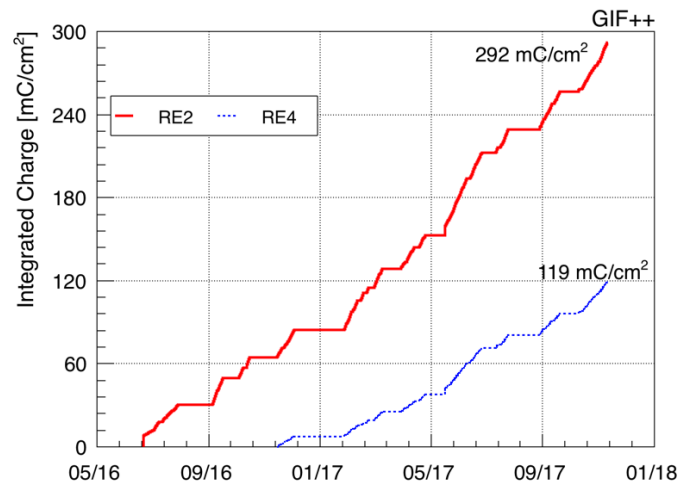

Figure 5. Integrated charge versus time collected during the GIF++ studies for the RE2/2 and RE4/2 chambers.

Since July 2016, several measurements with tests beams have been performed. The efficiency and the cluster size of all four RPCs has been measured in several background conditions, using the removable filters in front of the ^{137}Cs gamma source that allow us to vary the background intensity from 0 to several kHz·cm^{-2}.

In figure 6, the hit efficiency of the RE2/2 chamber as a function of the effective HV (voltage normalized at the standard temperature and pressure) is reported for various periods of radiation at GIF++ with no irradiation (left) and with a gamma background rate of 600 Hz·cm^{-2} (right). The method for the data analysis is described in ref. [13]. No signs of aging have been observed so far. The working point, defined as the voltage at which 95% of the maximum efficiency is reached,

is unchanged after different periods of irradiation, both under $600 \, \mathrm{Hz \cdot cm^{-2}}$ and without gamma background rate. The measurements show no reduction in the hit efficiency and the working points are unchanged after different values of integrated charge.
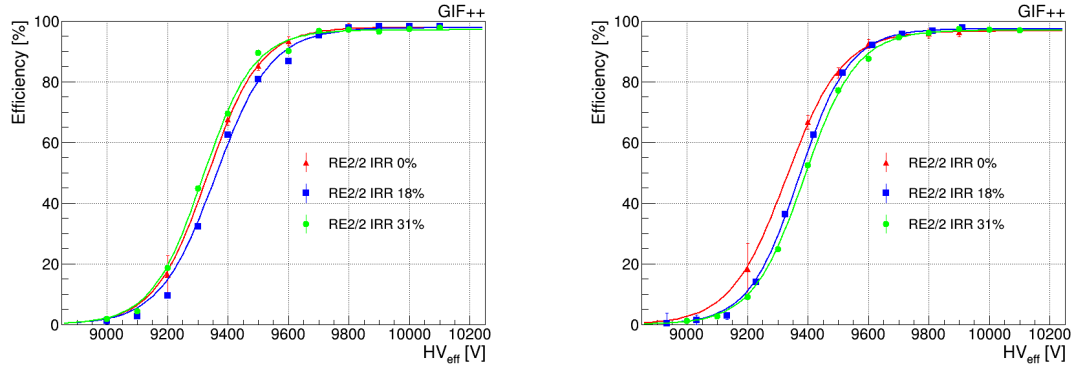

Figure 6. RE2/2 hit efficiency as a function of the effective HV taken with no irradiation (left) and under gamma background rate of about $600 \, \mathrm{Hz \cdot cm^{-2}}$ (right). No significant variations have been observed in the detector performance.

The hit efficiency and the cluster size for both irradiated and the nonirradiated RE2/2 chambers at the working point as a function of the background rate are shown in figure 7. For all detectors the efficiency is stable in time with a small decrease (2%) of the efficiency at the highest expected background rate of $600 \, \mathrm{Hz \cdot cm^{-2}}$. The measurement was repeated after different periods of irradiation corresponding to 18% ($153 \, \mathrm{mC \cdot cm^{-2}}$) and 31% ($260 \, \mathrm{mC \cdot cm^{-2}}$) of the total integrated charge target.

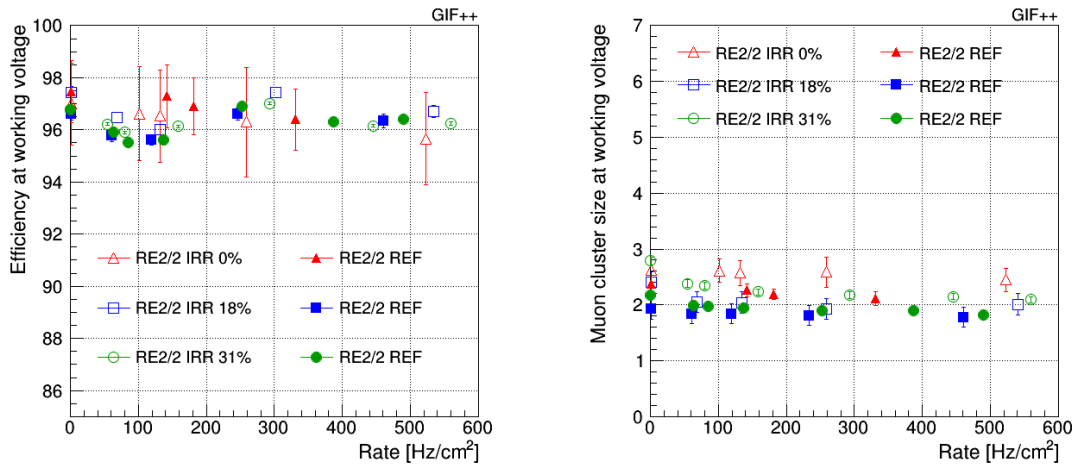**Figure 7**. Measurement of the hit efficiency (left) and cluster size (right) at the working point for RE2/2 chambers as a function of the γ rate per unit area. Both irradiated and reference chambers are shown. The measurements have been repeated after different periods of irradiation corresponding to 18% and 31% of the total integrated charge expected by the end of HL-LHC.

The stability of the system is studied by monitoring the rate and the RPC current, for both irradiated and nonirradiated reference chambers. To cancel out the dependence on the environmental
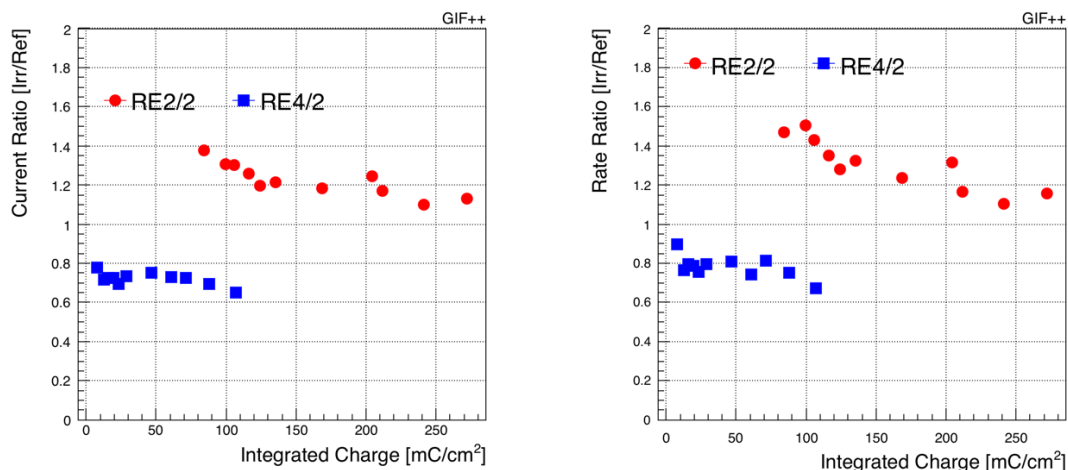
Figure 8. Current (left) and rate (right) ratio between irradiated and nonirradiated reference chambers as a function of the integrated charge. Circles correspond to RE2/2 chambers, squares to RE4/2.

conditions, the ratio of irradiated and reference chambers is measured as a function of the integrated charge as shown in figure 8. The difference in the ratio between the two chambers is due to the different relative position of RE2/2 and RE4/2 chambers with respect to the reference chambers inside the GIF++ test zone. The measurements show a stable performance of the detectors with a decrease at the beginning of the irradiation period. This decrease can be explained as an electrode resistivity increase due to the low levels of gas flow rate and humidity [14] with respect to the background rate conditions of $1 \, \text{kHz} \cdot \text{cm}^{-2}$.

6 Summary

Two CMS RPC double-gap endcap chambers were irradiated with the goal of accumulating an integrated charge of $840 \, \text{mC} \cdot \text{cm}^{-2}$. The performance and the stability of the detectors were measured as a function of HL-LHC background rates and for various fractions up to one-third of the total integrated charge expected at the end of the HL-LHC. At this point, we observe no sign of performance degradation at the expected high background rates and no aging was observed. Further measurements are needed to achieve the final integrated charge requirements proposed for the longevity study of the present CMS RPC system.

References

[1] CMS collaboration, *The CMS Experiment at the CERN LHC*, 2008 *JINST* **3** S08004.

[2] CMS collaboration, *The CMS muon project: Technical Design Report*, CERN-LHCC-97-032 (1997).

[3] L. Evans and P. Bryant, *LHC Machine*, 2008 *JINST* **3** S08001.

[4] G. Apollinari et al., *High-Luminosity Large Hadron Collider (HL-LHC): Preliminary Design Report*, CERN-2015-005 (2015).

[5] G. Apollinari et al., *High-Luminosity Large Hadron Collider (HL-LHC), Technical Design Report*, CERN-2017-007-M (2017).

[6] M. Abbrescia et al., *Study of long-term performance of CMS RPC under irradiation at the CERN GIF*, *Nucl. Instrum. Meth.* **A 533** (2004) 102.

[7] H.C. Kim et al., *Quantitative aging study with intense irradiation tests for the CMS forward RPCs*, *Nucl. Instrum. Meth.* **A 602** (2009) 771.

[8] D. Pfeiffer, G. Gorine, H. Reithler, B. Biskup, A. Day, A. Fabich et al., *The radiation field in the Gamma Irradiation Facility GIF++ at CERN*, *Nucl. Instrum. Meth.* **A 866** (2017) 91 [arXiv:1611.00299].

[9] CMS collaboration, *Performance of the CMS muon detector and muon reconstruction with proton-proton collisions at $\sqrt{s} = 13\,TeV$*, 2018 *JINST* **13** P06015 [arXiv:1804.04528].

[10] CMS collaboration, *The Phase-2 Upgrade of the CMS Muon Detectors*, CERN-LHCC-2017-012 (2017).

[11] S. Costantini et al., *Radiation background with the CMS RPCs at the LHC*, 2015 *JINST* **10** C05031 [arXiv:1406.2859].

[12] M.I. Pedraza-Morales, M.A. Shah and M. Shopova, *First results of CMS RPC performance at 13 TeV*, 2016 *JINST* **11** C12003 [arXiv:1605.09521].

[13] M. Abbrescia et al., *Cosmic ray tests of double-gap resistive plate chambers for the CMS experiment*, *Nucl. Instrum. Meth.* **A 550** (2005) 116.

[14] R. Arnaldi et al., *Influence of temperature and humidity on bakelite resistivity*, *Nucl. Instrum. Meth.* **A 456** (2000) 140.